



1 **Parameter dynamics of distributed hydrological model in simulating**
2 **or forecasting flood processes of urbanizing watersheds**

3

4

Yangbo Chen^{1*}, Jun Liu¹, Liming Dong¹

5

6

¹School of Geography and Planning, Sun Yat-sen University, Guangzhou 510275,
7 China

8

9

Correspondence to: Yangbo Chen (eescyb@mail.sysu.edu.cn), +86-138-26161264

10

11 **Abstract:** In the past decades, the world has experienced rapid urbanization and
12 observed the appearances of large amount urbanizing watersheds with enhanced
13 flooding, which has a constant changing land use/cover(LUC) types as the most
14 significant feature. Simulating and forecasting urbanizing watershed flood processes
15 faces great challenges, one is how to relate model parameters with the changing LUCs
16 to secure an accurately and reliable simulation and forecasting results. In this study, a
17 methodology for simulating and forecasting urbanizing watershed flood processes is
18 proposed, which employs Liuxihe model as the watershed hydrological model. This
19 methodology sets up the Liuxihe model with latest terrain properties, then derives
20 initial parameter look-up table based on terrain properties, and optimizes it if there is
21 observed hydrological data. If there is LUC changes, then the parameters are updated
22 with the changed LUCs based on the optimized parameter look-up tables. Case study
23 in a highly urbanizing watershed in the Pearl River Delta Area in southern China has
24 shown that this method acquires accurate and reliable flood processes simulation
25 results. Further more, this study has proven an assumption that the hydrological model
26 parameters are LUC stationary, i.e., with the LUC changes, the parameter look-up
27 table will not change, parameter look-up table optimized in a specific time with
28 current LUCs will not change even the LUCs changed. With this assumption, the
29 parameter look-up table only needs to be optimized once. This is a science question
30 that has not been not well answered yet by the scientific communities.

31

32 **Keywords:** Flood simulation, flood forecasting, land use/cover change, Liuxihe model,
33 parameter optimization



34 **1 Introduction**

35 In this study, an urbanizing watershed is referred to a watershed with constant land
36 use/cover (LUC) changing, and has urban land (impervious surface) as its major or
37 significant LUC type. Urbanizing watersheds usually locate in the rapidly developing
38 or urbanizing area. For the past century, the world is in constant urbanization (He et
39 al., 2021; Addae and Dragicevic, 2023), and its urban population reached 50% in
40 2007 (United Nations, 2014). While for the developing countries, the urbanization
41 trend is still rapidly going (Huang et al., 2022; Xue et al., 2022). For example, intense
42 urbanization has occurred in India and Nigeria from 1970-2010, where 85% and 30%
43 of cropland area within ten km of urban areas converted to urban land respectively
44 (Gunalp et al., 2020). China also experienced a rapid urbanization since 1978, with
45 its urban population reached 55% in 2018 (Zhao et al., 2023; Fang and Wang, 2011).
46 China's urbanization is still going on and quick in some regions (Yu, 2021), with its
47 urban population projected to be 68% in 2050 (Development Research Foundation of
48 China, 2010). During this world urbanization process, lots of urbanizing watersheds
49 appeared worldwide, some of them already have very high urban land percentage over
50 50% (Wang and Chen, 2019), while others are still in its growing stage. For example,
51 in China's Pearl River Delta Area (PRDA) where the rapidest regional urbanization
52 was observed in China (Li et al., 2011), most of the watersheds have a higher than
53 30% urban land rate, with some over 50% already (Chen et al., 2015, Zhang et al.,
54 2015).

55



56 For an urbanizing watershed, rapid land use/cover (LUC) change, particularly the
57 converting of vegetated area (pervious surface) into urban land area (impervious
58 surface), is the most observed direct change caused by human activities. This change
59 induces increased surface runoff and peak flow, which was well observed and analyzed
60 (Leopold, 1968; Hollis, 1975; Rose et al., 2001; Yang et al., 2016; Wang et al., 2022;
61 Zhao et al., 2023). Simulating watershed flood processes has long been the goal of the
62 world hydrological communities, it is the prerequisite for flood mitigation project
63 design and flood forecasting. But for an urbanizing watershed, how to consider the
64 LUCs change in the simulation is still a great challenge.

65

66 Watershed hydrological models are the most employed tools for watershed flood
67 processes simulation and forecast, lumped models are widely used in the early stages
68 (Refsgaard et al., 1996; Chen et al., 2011), such as the Stanford model (Crawford et al.,
69 1966), the Xinanjiang model (Zhao, 1977) and the ARNO model (Todini, 1996), only
70 list a few. Lumped models calibrate model parameters by using series hydrological data
71 observed in the past, and the LUC change could not be reflected with model structure
72 or parameter, thus can only be used for simulating the past hydrological processes, not
73 the changing one. For this reason, lumped hydrological models are not the appropriate
74 models for simulating or forecasting urbanizing watersheds flood.

75

76 Physically based distributed hydrological models (PBDHMs) are the new
77 development of watershed hydrological models, as the terrain is divided into grid cells
78 (Freeze and Harlan, 1969; Abbott et al., 1986a, 1986b) and the runoff production and
79 routing are calculated cell by cell, thus having the potential to better simulate



80 hydrological processes (Ambroise et al., 1996). Dozens of PBDHMs have been
81 proposed and widely used in scientific studies, including the SHE model (System
82 Hydrologue Europeen model) (Abbott et al., 1986a, b), the VIC model (variable
83 infiltration capacity model) (Liang et al., 1994), the WEP model (Water and Energy
84 transfer Process model) (Jia et al., 2001) and the Liuxihe model (Chen et al., 2011),
85 and many others. The most outstanding feature of PBDHMs is that model parameters
86 have physical meanings, and can be directly derived from the watershed terrain
87 properties, such as the elevation, soil type and LUC. A table is usually set up to define
88 the relationship between the parameters and the terrain properties, which is referred to
89 as the parameter look-up table. This gives PBDHMs potential to simulate or forecast
90 urbanizing watershed flood as it can relate model parameters with LUC changes.

91

92 In the early study, look-up table is proposed based on limited local experiences and
93 laboratory experiments, which shows big uncertainty and impacts the model's
94 performance. Recent studies have shown that parameter optimization can improve
95 PBDHMs performances (Madsen, 2003; Smith et al., 2004; Pokhrel et al., 2012; Chen
96 et al., 2016), which was assumed previously that parameter optimization is not needed
97 for PBDHMs. Several methods have been proposed, such as the scalar method (Vieux
98 et al., 2003; Vieux, 2004) for Vflo model, the SCE algorithm for MIKE SHE (Madsen,
99 2003), the multi-objective genetic algorithm for WetSpa model (Shafii et al., 2009), the
100 SCE-UA algorithm (Xu et al., 2012) and the Particle Swam Optimization (PSO)
101 algorithm (Chen et al., 2016) for Liuxihe model. But these efforts were mainly carried
102 out in simulating or forecasting flood for natural watershed, i.e., watershed with little
103 LUC changes.



104

105 For simulating or forecasting urbanizing watershed flood processes by using a PBDHM,
106 big challenges still exist. The biggest one is how to acquire a reliable and accurate look-
107 up table, so to adjust parameters with changing LUCs. The second is a science question,
108 i.e., if a reliable and accurate look-up table could be set up, then should it be LUC
109 stationary? I.e., with the LUC changing, the look-up table should be changed
110 accordingly or not? There are two purposes for this study, the first is to propose a
111 methodology for simulating or forecasting urbanizing watershed flood processes by
112 using a PBDHM with satisfactory model performances, which can relate the model
113 parameters with the changing LUCs. This methodology employs Liuxihe model as the
114 PBDHM, and sets up the Liuxihe model with latest terrain properties; then proposes an
115 initial parameter look-up table based on current parameterization experiences, and
116 optimizes it if there is observed hydrological data. With parameter look-up table
117 optimization, the parameter look-up table is reliable and accurate. This methodology
118 solves the first challenge and has been tested in a highly urbanized watershed in southern
119 China.

120

121 The second purpose is to answer the science question of parameter stationary. The
122 authors assume that the model parameters are LUC stationary, i.e., with the LUC
123 changing, the parameter look-up table will not change, i.e., a parameter look-up table
124 optimized in a specific time with current LUCs will not change after the LUCs changed.
125 With this assumption, the parameter look-up table only needs to be optimized once.
126 This assumption has been proven by the simulation results in the case study, so to solve
127 the second challenge. The remaining parts of this article are organized into 4 sections.
128 Section 2 introduces the study watershed, the hydrological data, LUC change data and



129 terrain property data. Section 3 introduces the methodologies, including Liuxihe model
130 and its parameter look-up table determination. Section 4 introduces the results in the
131 case study watershed, and section 5 provides a discussion.

132 **2 Study watershed and data**

133 **2.1 Study watershed**

134 Songmushan Watershed(SW) is the upstream of Hanxishui River Basin(HRB) locating
135 in Dongguan City in southern China. Songmushan Reservoir(SR) was built in the
136 middle stream of SW, and the watershed area controlled by SR is called as Songmushan
137 Reservoir Watershed (SRW) in this study. Originating from the Lotus Mountain, SRW
138 has a drainage area of 54.2 km², and a river length of 11.19 km. SRW was selected as
139 the study watershed because it is a typical urbanizing watershed in China, and
140 hydrological data in recent years for this study is also available. Fig. 1 shows the
141 location of SRW.

142

143 Fig. 1 is here

144

145 The major topography of SRW is gentle hills. This area enjoys a subtropical monsoon
146 climate with frequent storms in the summer monsoon season. Average annual
147 precipitation of SRW is 1674 mm, which caused serious flooding in the past. SRW has
148 observed rapid urbanization in the past decade, which has created a high percentage of
149 urbanized land. It is a typical watershed in the Pearl River Delta area that experiences
150 considerable increasing both in flooding and urbanization.

151

152 Songmushan Reservoir was initially built for irrigation in 1958 as Dongguan City was



153 primarily an agriculture area at that time, and there was no systematical hydrological
154 observation until 2008. With China's reforming and opening, Dongguan City has been
155 developing very fast since 1987, and become an international metropolitan. Dongguan
156 City has been a highly urbanized area since then, and there is almost no agriculture
157 anymore. For this reason, irrigation is not needed, and the reservoir has the new roles
158 of flood mitigation and water supply after a heavy flooding in 2006. In 2008, an
159 automatic hydrological data collecting system was built which includes 6 rain gauges
160 (Fig. 1) and 1 water level gauge at the dam site.

161 **2.2 Hydrological data**

162 In this study, hydrological data of 13 flood events between 2008 and 2015 was obtained,
163 including precipitation of the 6 rain gauges and the reservoir inflow at one hour interval.
164 Table 1 shows the basic information of these flood events.

165

166 Table 1 is here

167 **2.3 LUC change data**

168 Chen et al. (2017) prepared a LUC dataset of the whole Dongguan City using the
169 Landsat series satellite remote sensing imagery (Irons et al., 2012, Tang et al., 2013). A
170 total of 12 imageries from 1987 to 2015 at an average 3-year interval were obtained,
171 and the SVM classifier algorithm (Vapnik, 1995) was employed to estimate the LUCs
172 accordingly. LUC data at 1987, 1990, 1993, 1996, 1999, 2001, 2003, 2005, 2008, 2011,
173 2013 and 2015 were prepared for the whole Dongguan City. There are six LUC types,
174 including urban land (impervious surface), water body, forestry land, farmland,
175 grassland and bare land. LUCs of SRW in 2008, 2011, 2013 and 2015 were extracted
176 from this dataset, Fig. 2 shows these results.

177



178 Fig. 2 is here

179

180 Urban land area of SRW was 18.62% in 2008, but reached 23.40%, 26.24% and 30.37%
181 in 2011, 2013 and 2015 respectively, this is a significant increasing in urban land under
182 urbanization, and this watershed could be regarded as an urbanizing watershed as its
183 LUCs was in constant changing from 2008 to 2015.

184 **2.4 Terrain property data**

185 Terrain property data is mainly used for model set up and initial model parameter
186 deriving, includes DEM, soil type and LUC type. DEM was prepared based on the
187 topography map surveyed recently by the local government agency, the spatial
188 resolution is at 30 m grid cell (Fig. 3(a)). The highest, lowest and mean elevation of the
189 watershed are 489 m, 9 m and 38.1 m respectively.

190

191 Soil map was downloaded from the FAO world soil map dataset (www.isric.org) as
192 shown in Fig. 3(b). There are 4 soil types in the watershed, including urban land, water
193 body, ferric Acrisols and cumulic Anthrosols, with areal percentages of 1.0%, 14.0%,
194 67.0% and 18.0% respectively.

195

196 Fig. 3 is here

197

198 In this study, a new soil type, the urban land soil type is defined. For which, its land
199 use/cover is the urban land, but its real soil type beneath the surface could be any type.
200 In fact, it is a virtual soil type proposed to facilitate the runoff production. So the soil
201 type data in Fig. 3(b) needs to be adjusted based on this definition. Besides, the urban
202 land data in Fig. 3(b) was prepared by FAO in 1990, so it is out of date, and have been



203 updated with the results of Fig. 2 in this study. The final soil types of SRW, adding the
204 urban land soil type, is produced and shown in Fig. 4, the soil types in 2018, 2011, 2013
205 and 2015 are different.

206 Fig. 4 is here

207 **3 Methodology**

208 **3.1 Liuxihe model**

209 The PBDHM employed in this study is the Liuxihe model, which is a physically based,
210 distributed hydrological model proposed for watershed flood forecasting (Chen, 2009;
211 Chen et al., 2011; Chen, 2017). But any PBDHMs which could relate its parameters
212 with LUCs could be employed.

213
214 Liuxihe model divides the watershed surface into grid cells, which are categorized as
215 hill slope cells, river channel cells and reservoir cells. For river channel cells and
216 reservoir cells, the watershed surface is water, runoff produced in these cells are equal
217 to the net precipitation. The surfaces of hill slope cells are covered with different land
218 use/cover (LUC) types, so each hill slope cell has its unique LUC. Currently in Liuxihe
219 model, there is no urban land LUC type, only vegetated LUCs. Each hill slope cell also
220 has its own soil type and elevation. LUC type, soil type and elevation are called
221 watershed terrain properties in Liuxihe model. Runoff is produced first on cells, and
222 then routed to the watershed outlet via a routing network. Runoff production is
223 governed by the infiltration, and the soil type is the controlling terrain property for
224 runoff production. Runoff routing is categorized as hill slope routing, river channel
225 routing and reservoir routing. The kinematical wave approximation is employed for hill
226 slope routing, while the diffusive wave approximation for river channel routing.

227



228 For Liuxihe model, there is no way to make runoff production and routing calculation
229 for the urban land grid cells, so in this study, a module that can make this calculation is
230 added. The urban land surface is impervious, the precipitation falls to this ground
231 surface is regarded completely converted into surface runoff, and no precipitation is
232 infiltrated to the soil beneath it. Runoff produced on cells with urban land surface is
233 equal to precipitation fallen to the surface. The approach used to calculate runoff
234 production is as below.

$$235 \quad R_{i,t} = P_{i,t} - E_{i,t} \quad (1)$$

236 Where $R_{i,t}$, $P_{i,t}$ and $E_{i,t}$ are surface runoff, precipitation and actual evaporation produced
237 on cell i at time t respectively, and the evaporation could be regarded as water surface
238 evaporation if there is surface runoff, otherwise it is zero.

239
240 As only the hill slope cell may have urban land surface, so the runoff routing on urban
241 land cell is hill slope routing. In Liuxihe model, hill slope routing is solved by using
242 kinematic wave approximation. For hill slope routing, the governing factors are the
243 slope of the cell and the roughness coefficient of the surface. For the hill slope routing
244 on urban land surface, the same approach is used but using different roughness
245 coefficient. The above approaches for runoff production and routing on urban land cell
246 has been developed and embedded into the currently used Liuxihe model software tool.

247 **3.2 Liuxihe model parameter look-up table determination**

248 Liuxihe model is a distributed hydrological model, so each grid cell has its own
249 parameters, i.e., 13 parameters (Chen et. al, 2011). The parameters in each grid cell are
250 divided into 4 categories, including climate-based parameters, topography-based
251 parameters, vegetation-based parameters and soil-based parameters (Chen et. al, 2016).
252 The parameters' values are related to only one category terrain property of its grid cell,



253 i. e., climate-based parameters are only related to the climate condition, the topography-
254 based parameters are only related to the topography, vegetation-based parameters are
255 only related to the land use/cover types, and the soil-based parameters are only related
256 to the soil types. There is only one climate-related parameter, i.e., the reference
257 evaporation which is regarded as the same for all grid cells. There are two topography-
258 based parameters, including flow directions and slopes for hill slope cells and river
259 channel cells. There are also two vegetation-based parameters, the evaporation
260 coefficient and roughness. There are 8 soil-based parameters, including soil property
261 coefficient, soil thickness, hydraulic conductivity under saturated condition, soil water
262 contents under saturated condition, field condition, and wilting condition. There is one
263 parameter for underground water routing which is regarded as the same for all grid cells,
264 and is also a soil-based parameter.

265

266 Liuxihe model takes two steps to determine model parameters, firstly deriving initial
267 parameter look-up tables from the watershed terrain property data, and then optimizing
268 them. For a specific watershed studied, Liuxihe model first proposes parameter look-
269 up tables, which are two-dimensional tables referring the values of parameters with the
270 terrain properties, for example, with soil type Ferric Acrisols, the parameter value of
271 soil water content under saturated conditions is referred to as 46.1%. Based on these
272 parameter look-up tables, the parameters of each grid cell could be determined
273 according to the grid cell's terrain properties, including DEM, LUCs and soil types. As
274 climate-based parameters take the same value for all grid cell, so there is no need for a
275 look-up table for the climate-based parameters. While the topography-based parameters
276 are calculated directly based on the DEM using the D8 method (O'Callaghan et al.,
277 1984; Jensen et al., 1988), so there is no need for a look-up table for the topography-



278 based parameters also. Therefor there are two parameter look-up tables, one is for
279 vegetation-based parameters, and another is for soil-based parameters.

280

281 Liuxihe model proposed ways for determining the two parameter look-up tables. For
282 the vegetation-based parameters look-up table, the referring values are decided from
283 laboratory experiments and local experiences, or even from references or results from
284 other watersheds. There are two vegetation-based parameters, the evaporation
285 coefficient and roughness. For the soil-based parameters look-up table, Liuxihe model
286 employs the Soil Water Characteristics Hydraulic Properties Calculator (Arya et al.,
287 1981) to calculate the referring values based on the soil texture, organic matter, gravel
288 content, salinity and compaction. With these parameters look-up table, based on its
289 terrain properties, the initial parameters for each grid cell could be derived. With this
290 way, if the terrain properties of each grid cell are available, then the initial parameters
291 could be proposed.

292

293 As the initial parameters derived with the above method are highly experience-based,
294 and current parameterization experiences are very limited, so the initial parameters have
295 uncertainty, thus model performance could not be secured. To improve model
296 performance, Liuxihe model optimizes the initial parameters by using optimization
297 algorithm, this is the second step of Liuxihe model parameters determination. From
298 past experiences of Liuxihe model parameterization, it has been found that parameter
299 optimization could largely improve the model's performance. Besides, in optimizing
300 model parameters, hydrological data from only one flood events is enough, not like
301 lumped hydrological mode, series of hydrological data is required. This is very
302 important for an urbanizing watershed as it usually has limited hydrological data, no



303 long series of hydrological data.

304

305 Currently two algorithms have been proposed for Liuxihe model parameter
306 optimization, one is SCE-UA algorithm (Xu et al., 2012), another is Particle Swam
307 Optimization (PSO) algorithm (Chen et al., 2016). In optimizing parameters, Liuxihe
308 model does not optimize all parameters of each grid cells, but optimizes the parameters
309 look-up tables. I.e., an adjusting coefficient for each terrain property is proposed, so the
310 optimized variables are limited, which makes the calculation practical, otherwise, even
311 with the fastest computers in the world, the optimization is not feasible.

312 **3.3 Dynamic parameter updating and parameter stationary**

313 For an urbanizing watershed, the terrain properties, particularly the LUCs are in
314 constant changes, so after parameter look-up table is optimized based on hydrological
315 data from one specific flood event and terrain properties at a specific date, model
316 parameters should be updated if the terrain properties changes, it is called in this study,
317 dynamic parameter updating, it is also the core concept of this study, that the model
318 parameters are dynamically changing with terrain property changes. Only with this
319 dynamic parameter updating, the model performance can be secured. But this parameter
320 updating is based on the assumption that the parameter look-up tables are LUCs
321 stationary, i.e., the look-up tables are not changed with the terrain property changing.
322 Otherwise, the updated parameters could not improve the model performance, or the
323 parameter look-up table needs to be optimized again with the changed LUCs and new
324 observed hydrological data.

325

326 Do the parameter look-up tables change with the watershed terrain property changing,
327 it is a science question that has not been answered and fully studied by the scientific



328 communities. The authors assume that the parameter look-up tables of Liuxihe model
329 are LUC stationary, and the simulation results in the case study will validate this
330 assumption.

331

332 **4 Results**

333 **4.1 Liuxihe model set up**

334 The DEM produced in this study with spatial resolution of 30 m is used to divide the
335 studied watershed into 62942 grid cells, which are further divided into 658 river cells,
336 53435 hill slope cells and 8849 reservoir cells, based on the method employed in
337 Liuxihe model. A 3-order river network is derived using the D8 method (O'Callaghan
338 et al., 1984; Jensen et al., 1988) and Strahler river ordering method (Strahler, 1957)
339 based on the DEM. The river network is further divided into 24 virtual sections based
340 on 4 virtual nodes. In the Liuxihe model, the virtual river cross section shape is
341 assumed trapezoidal, and the river size is estimated based on satellite remote sensing
342 images. The structure of the Liuxihe model for SRW set up in this study is shown in
343 Fig. 5. The time resolution of the Liuxihe model set up in SRW is 1 hour, the same
344 with that of the observed hydrological data. Precipitation from rain gauges is
345 interpolated to the grid cells by using the Thiessen Polygon method (Thiessen, 1911).

346

347 Fig. 5 is here

348

349 Flow directions and slopes are derived using the D8 method (O'Callaghan et al., 1984,
350 Jensen et al., 1988) based on the DEM. The climate-based parameter, i.e., the potential
351 evaporation is estimated as 5 mm/day for each grid cell according to daily evaporation
352 observations in this region. According to previous studies of Liuxihe model



353 parameterization and references (Chen et al., 1995; Zhang et al., 2006, 2007; Guo et al.,
354 2010; Li et al., 2013), the initial look-up table for vegetation-based parameters is
355 proposed and listed in Table 2.

356

357 Table 2 is here

358

359 Based on past modeling studies (Zaradny, 1993; Anderson et al., 1996; Shen et al., 2007;
360 Zhang et al., 2015), the soil water content under wilting conditions takes 30% of the
361 soil water content under field conditions, and the soil porosity coefficient takes the
362 value of 2.5. Based on local experiences, the estimated soil layer thickness is listed in
363 Table 3. The Soil Water Characteristics Hydraulic Properties Calculator proposed by
364 Arya et al. (1981) is employed to calculate the soil water contents under saturation
365 condition and field condition, and the hydraulic conductivity under saturation
366 conditions, as listed in Table 3.

367

368 Table 3 is here

369

370 For grid cells with urban land soil type, all the soil-based parameters are set to zero.
371 This reflects the hydrological response of urban land soil type, i.e., the precipitation
372 falling onto urban land will be converted into surface runoff completely, no
373 precipitation will be infiltrated to the soil or stored on the surface.

374

375 For Liuxihe model, hydrological data from only one flood event is needed for parameter
376 optimization, and Particle Swarm Optimization(PSO) is the official optimization
377 algorithm, which has been tested and proven to be effective. In this study, hydrological



378 data from flood event 20080625 is used for parameter optimization, and PSO algorithm
379 is employed to optimize the parameters, while LUCs in 2008 is used. The optimized
380 parameter look-up tables are called parameter-20080625-2008 to distinguish
381 parameters optimized with different hydrological data and LUCs in different year. In
382 parameter-20080625-2008, the first number is the flood event number with its
383 hydrological data being used for parameter optimization, while the second one is the
384 year of the LUCs which is used in the parameter optimization. I.e., Parameter-
385 20080625-2008 is the optimized parameters by using hydrological data from flood
386 event 20080625 and LUCs in 2008. Fig. 6 shows the evolution results of parameters,
387 adaptive values and evaluation indices during the parameter optimization process.

388

389 Fig. 6 is here

390

391 With 9 evolution, the model parameters approached their optimal values, and the
392 simulated hydrograph with optimized parameters fits the observed flood event well as
393 shown in Fig 6(d), this means the PSO algorithm has good performance for Liuxihe
394 model parameter optimization.

395

396 From the result of Fig 6(a), it has been found that the initial value of soil property
397 coefficient is quite different from its optimized value, but with the optimization of PSO
398 algorithm, its optimized value is obtained, this implies that the PSO algorithm has good
399 convergence, and well suits Liuxihe model parameter optimization.

400 **4.2 Flood simulation with Parameter-20080625-2008**

401 With the above optimized Parameter-20080625-2008, the other 12 flood events were
402 simulated, while in this simulation, the LUCs in 2018 are used for all the 12 flood



403 events, that means the parameters are regarded not changed during the watershed
404 urbanization, and the model parameters are not updated dynamically with the LUC
405 changing. Four evaluation indices, including Nash-Sutcliffe coefficient, mean relative
406 error, peak flow error and peak flow timing error, has been calculated and listed in Table
407 4, the simulated hydrographs are shown in Fig. 7.

408

409 Table 4 is here

410

411 Fig. 7 is here

412

413 From the results shown in Table 4 and Fig. 7, it has been found that for all the 12 flood
414 events, the simulated hydrographs are similar with the observations in shape. In average
415 for all the 12 flood events, the Nash-Sutcliffe coefficient is 0.79, the mean relative error
416 is 63.91%, the peak flow error is 19.47%, while the peak flow timing error is -0.58 hour.
417 From these results, the flood processes of SRW have been simulated reasonable by
418 Liuxihe model set up in this study.

419

420 From the above results, we also find that the four evaluation indices get worse with
421 time goes. For example, the average peak flow error for flood events in 2008 and 2009
422 is 6.7%, 35.88% in 2011, 17.15% in 2013 and 2014, and 27.87% in 2015, in general,
423 the average peak flow error gets bigger as time goes. For the Nash-Sutcliffe coefficient,
424 those in 2008 and 2009, in 2011, in 2013 and 2014, and in 2015 are 0.835, 0.775, 0.753
425 and 0.76, a similar trend with peak flow error. Based on these results, it can be proposed
426 that the model parameters should have changed with time going, i.e., with LUC changes,
427 and the model parameters need to be adjusted with the changing LUCs. To verify this



428 opinion, the dynamical parameter updating is tested in the follow-up section.

429

430 **4.3 Flood simulation with dynamic updating to parameter-20080625-2008**

431 Based on the dynamic parameter updating method proposed in this study, parameters
432 used for simulating flood events in 2011, in 2013 and 2014, in 2015 are updated with
433 the LUCs in 2011, 2013 and 2015 respectively based on parameter-20080625-2008.
434 The dynamically updated model parameters in 2011, 2013 and 2015 are different from
435 each other, so are from parameter-20080625-2008, which is called parameter-
436 20080625-2008-updated. With these parameters, 8 flood events(parameters for the
437 flood events in 2008 and 2009 are not updated) are simulated again, the four evaluation
438 indices have been calculated and listed in Table 5, the simulated hydrographs are shown
439 in Fig. 7 also to make comparison with those results simulated with no parameter
440 updating.

441

442 Table 5 is here

443

444 From the results shown in Fig. 7 and Tabel 5, it has been found that the model
445 performance has been improved with dynamic parameter updating. For example, for all
446 the 8 flood events, the simulated hydrographs fit those of the observations better than
447 those simulated with no parameter updating. The Nash-Sutcliffe coefficients of all the
448 simulated flood events with updated parameters gets higher, except those of flood event
449 no. 20150520 and 20150720. The average Nash-Sutcliffe coefficient increasing is 0.764,
450 a 0.3% increasing. While for the peak flow error, all flood events have observed
451 decreasing, the average decreasing is 66.81%, a very significant model performance
452 imporvement. These results imply that with dynamical parameter updating, Liuxihe



453 model has a much better performance in simulating the flood events of SRW, i.e., model
454 parameters are in dynamic changing with the LUC changing, and dynamical parameter
455 updating with the LUC changing is needed. This confirms the dynamic characteristics
456 of model parameters.

457

458 **5 Discussions**

459 **5.1 Effect of parameter optimization on model performance**

460 To test the effectiveness of parameter optimization, the 12 flood events are simulated
461 with the initial parameters, and the results are shown in Fig 8, to make comparison, the
462 simulated hydrographs with dynamically updated parameters are also shown. From the
463 results it could be found that the simulation results with initial and dynamically updated
464 parameters are quite different. Though both the simulated hydrographs have similar
465 patterns, but the flows simulated with the initial parameters are generally much lower
466 than the observations, and those simulated with the dynamically updated parameters
467 well fit the observation.

468

469 Fig. 8 is here

470

471 The four evaluation indices of the 12 flood events is calculated and listed in Table 6.
472 Compared with the simulation with initial parameter, the simulation with dynamically
473 updated parameters has been improved much based on these evaluation indices. Among
474 them, the average Nash-Sutcliffe coefficient increased 68.2%, correlation coefficient
475 increased 3.2%, peak flow error reduced 86.4%, water balance coefficient increased
476 45.8%. These results show that parameter optimization is needed and feasible even for
477 distributed hydrological model.



478

479

Table 6 is here

480

481 **5.2 Parameter stationary**

482 In above sections, the dynamic parameter updating was based on the optimized
483 parameter look-up tables with LUCs in 2018. There appears a question, should the look-
484 up table be optimized with the latest LUCs, not the LUCs at a specific time? I.e., is the
485 look-up table no-stationary to LUCs during urbanization. If yes, then the look-up table
486 needs to be optimized with the latest LUCs, and done again when there is significant
487 LUC change. Otherwise, the look-up table can be optimized with LUCs at any time,
488 and there is no need to optimize it very often. To answer this question, in this study, the
489 parameters were optimized with LUCs in 2011, 2013 and 2015 also, and the
490 hydrological data used for parameter optimization were from flood events 20110516,
491 20130815 and 20150520 respectively, these parameters are called parameter-
492 20110516-2011, parameter-20130815-2013, and parameter-20150520-2015
493 respectively. Then the parameters are dynamically updated with latest LUCs, and are
494 called parameter-20110516-2011-updated and parameter-20130815-2013-updated
495 respectively, there is not parameter-20150520-2015-updated. I. e., dynamical parameter
496 updating is time forward, not time backward. For example, parameter-20110516-2011-
497 updated only update parameters with LUCs in 2013 and 2015, not in 2008 and 2011;
498 parameter-20130815-2013-updated only update parameters with LUCs in 2015, not in
499 2008, 2011 and 2013, so there is not parameter-20150520-2015-updated. The
500 dynamically optimized and updated parameters are then employed to simulate the flood
501 events, and the results are shown in Fig. 9. The four evaluation indices are calculated
502 and listed in table 7.



503

504

Table 7 is here

505

506

Fig. 9 is here

507

508 Both the simulated flood hydrographs with and without dynamic parameters optimizing
509 and updating have no obvious differences, so based on the above methods and results,
510 it can be concluded that the parameters are stationary during the urbanization, i.e.,
511 during the LUC changing period. There is no need to optimize the look-up table very
512 often with rapid LUC changing, parameter optimization and updating is most important.

513 **5.3 Impact of LUC changes on flood responses**

514 Based on the above results, it could be found that with the LUC changes, the flood
515 response changes also. To quantitatively analysis this effect, the peak flow and urban
516 land area rate of flood events from 2011 to 2015 are extracted from the above results
517 and listed in Table 8. The values with no-update are the simulated values with
518 parameter-20080625-2008, while the ones with update are the simulated values with
519 parameter-20080625-2008-update.

520

521

Table 8 is here

522

523 From the results, it could be found that from 2008 to 2011, the SRW observed an urban
524 land rate change from 18.62% to 23.4%, a 25.67% increasing. For flood event
525 20110516, with the same precipitaion, the peak flow will change from 87.08 m³/s to
526 99.42 m³/s, having a 14.2% increasing. While for flood event 201100808, the peak flow
527 change is from 103.68 m³/s to 117.21 m³/s, having a 13.1% increasing. Both these
528 events are light flood, the peak flow increasing has similar magnitude.



529 But from 2008 to 2013, the SRW observed an urban land rate increasing of 40.92%.
530 For flood event 20130815, which is regarded as a heavy flood event, the peak flow
531 increasing is 9.0%, while for flood event 20140511, the peak flow increasing is 12.8%,
532 for flood event 20140819, this is 14.6%. The latter two flood events are regarded as
533 medium. With these results, it can be concluded that the much heavier of the flood
534 magnitude, the more increasing of peak flow.

535

536 From 2008 to 2015, the SRW observed an urban land rate increasing of 63.10%. For
537 flood event 20150520, which is regarded as a light flood event, and flood events
538 20150523 and 20150720, which are regarded as a medium flood event, the peak flow
539 increasing are 56.3%, 18.5%, and 12.2% respectively. This implies that for the light
540 flood event, the peak flow increases much more. Based on this analysis, with the
541 increasing of the urban land area rate, the peak flow of a flood event will increase, and
542 the light flood event has the most peak flow increasing, while the heavy one has the
543 least peak flow increasing.

544

545 **6 Conclusions**

546 In this study, a method is proposed for accurately simulating flood processes of
547 urbanizing watersheds that appear during the world urbanization process, which
548 employs the Liuxihe model, a physically based distributed hydrological model as the
549 flood simulation tool. This method first derives initial parameter look-up tables, and
550 then optimizes it, and dynamically updates the parameter with the changing LUCs to
551 improve the model performance. A case study has been carried out in the Songmushan
552 Reservoir Watershed, a highly urbanizing watershed in the Pearl River Delta Area in
553 southern China which experienced rapid urbanization in the past decade. Based on the
554 results, following conclusions have been proposed.



555

556 1. The methodology proposed in this study could be used for simulating and forecasting
557 urbanizing watershed flood processes with good model performance.

558

559 2. For an urbanizing watershed, terrain properties are in changing, and model
560 parameters are in changing also due to terrain properties changing, this is called
561 model parameter dynamics. Model parameters should be updated with the LUC
562 changes.

563

564 3. Parameter look-up table of physical based distributed hydrological model is LUC
565 stationary, i.e., the parameter look-up table only needs to be determined once during
566 the watershed urbanization.

567

568 4. With same precipitation, flood peak flow will increase due to urban land rate
569 increases. The much heavier the precipitation, the less increasing of the peak flow.

570

571 5. Parameter optimization is effective and needed in controlling parameter uncertainty
572 for physically based distributed hydrological model.

573

574 **Competing interests:** The contact author has declared that none of the authors
575 has any competing interests.

576



577 **Acknowledgements:** This study was supported by the National Natural Science
578 Foundation of China (NSFC) (no. 51961125206), and the Science and Technology
579 Program of Guangdong Province (no. 2020B1515120079).
580



581 References

- 582 [1] Abbott, M. B., J. C. Bathurst, J. A. Cunge, P. E. O E. O J. C. Bathurst, J. A. Cunge,
583 P. E. Oting the Twentieth Five-year Plan Period ter optHydrologue Europeen,
584 'SHE', a: History and Philosophy of a Physically-based, Distributed Modelling
585 System. *J. Hydrol.*, 87, 45-59.
- 586 [2] Abbott, M. B., J. C. Bathurst, J. A. Cunge, P. E. O E. O J. C. Bathurst, J. A. Cunge,
587 P. E. Otributed Modelling System. *J. lan Period ter optHydrologue Europeen*,
588 'SHE', b: Structure of a Physically based, distributed modeling System. *J. Hydrol.*,
589 87, 61-77.
- 590 [3] Addae, B. and Dragicevic, S.: Modelling global urban land-use change process
591 using spherical cellular automata, *Geojournal*, 88, 2737-2754, 10.1007/s10708-
592 022-10776-4, 2023.
- 593 [4] Ambrose, B.; Beven, K.; Freer, J. Toward a generalization of the TOPMODEL
594 concepts: Topographic indices of hydrologic similarity. *Water Resour. Res.* 1996,
595 32, 2135–2145.
- 596 [5] Anderson, A. N., A. B. McBratney and K. E. FitzPatric, 1996. A soil mass, surface
597 and spectral fractal dimensions estimated from thin section photographs. *Soil Sci.*
598 *Soc. Am. J.*, 60, 962-969.
599 <https://doi.org/10.2136/sssaj1996.03615995006000040002x>
- 600 [6] Arya, L.M., and J. F. Paris, 1981. A physioempirical model to predict the soil
601 moisture characteristic from particle-size distribution and bulk density data. *Soil*
602 *Sci. Soc. Am. J.*, 45, 1023-1030.
603 <https://doi.org/10.2136/sssaj1981.03615995004500060004x>
- 604 [7] Chen H, Mao S. 1995. Calculation and Verification of an Universal Water Surface
605 Evaporation Coefficient Formula. *Advances in Water Science* 6(2):116-120.
606 <https://doi.org/10.14042/j.cnki.32.1309.1995.02.005>
- 607 [8] Chen, Y., 2009. *Liuxihe Model*, Beijing, Science Press, 198 pp.
- 608 [9] Chen, Y., Q. W. Ren, F. H. Huang, H. J. Xu, and I. Cluckie, 2011. *Liuxihe Model*
609 *and its modeling to river basin flood*. *J. Hydr. Eng.*, 16, 33-50.
- 610 [10] Chen, Y., H. Zhou, H. Zhang, G. Du, J. Zhou, 2015. Urban flood risk warning
611 *under rapid urbanization*, *Environmental Research* 139(5):3-10.
- 612 [11] Chen, Y., J. Li, and H. Xu, 2016. Improving flood forecasting capability of
613 *physically based distributed hydrological model by parameter optimization*.
614 *Hydrol. Earth Syst. Sci.*, 20, 375-392. <https://doi.org/10.5194/hess-20-375-2016>
- 615 [12] Chen, Y., 2017. Distributed Hydrological Models, in *Handbook of*
616 *Hydrometeorological Ensemble Forecasting*, Q. Duan et al. (eds.), 1-12,
617 https://doi.org/10.1007/978-3-642-40457-3_23-1.
- 618 [13] Chen, Y., T. Zhang, P. Dou, L. Dong, and H. Chen, 2017. Error sources and post
619 *processing method for land use/cover change estimation of Dongguan City based*
620 *on Landsat remote sensing imagery with SVM*, *Remote Sensing Technology and*
621 *Application*, in press. <https://doi.org/10.11873/j.issn.1004-0323.2017.5.0893>
- 622 [14] Crawford, N. H., and R. K. Linsley, 1966. Digital simulation in hydrology,
623 *Stanford Watershed Model IV*. Stanford Univ. Dep. Civ. Eng. Tech. Rep. 39.
- 624 [15] Development Research Foundation of China, 2010. *Development Report of*
625 *China*. People's Publishing, Beijing.
- 626 [16] Fang, C., D. Wang, 2011. Comprehensive development measuring and improving
627 *roadmap of China's urbanization quality*. *Geogr. Res.* 30(11):1931-1945.
628 <https://doi.org/10.3724/SP.J.1011.2011.00211>



- 629 [17] Freeze, R. A., and R. L. Harlan, 1969. Blueprint for a physically-based, digitally
630 simulated, hydrologic response model. *J. Hydrol.*, 9, 237-258.
631 [https://doi.org/10.1016/0022-1694\(69\)90020-1](https://doi.org/10.1016/0022-1694(69)90020-1)
- 632 [18] Guo, H., Y. Hua, X. Bai, 2010. Hydrological Effects of Litter on Different Forest
633 Stands and Study about Surface Roughness Coefficient. *Journal of Soil and Water*
634 *Conservation*, 24(2), 179-183. <https://doi.org/10.3724/SP.J.1238.2010.00474>
- 635 [19] Guneralp, B., Reba, M., Hales, B. U., Wentz, E. A., and Seto, K. C.: Trends in urban
636 land expansion, density, and land transitions from 1970 to 2010: a global synthesis,
637 *Environmental Research Letters*, 15, 10.1088/1748-9326/ab6669, 2020.
- 638 [20] He, C., Liu, Z., Wu, J., Pan, X., Fang, Z., Li, J., and Bryan, B. A.: Future global
639 urban water scarcity and potential solutions, *Nature Communications*, 12, 4667,
640 10.1038/s41467-021-25026-3, 2021.
- 641 [21] Hollis, G. E., 1975. The effect of urbanization on floods of different recurrence
642 interval. *Water Resour. Res.*, 11(3), 431-435.
643 <https://doi.org/10.1029/WR011i003p00431>
- 644 [22] Huang, J., Yang, Y., Yang, Y., Fang, Z., and Wang, H.: Risk assessment of urban
645 rainstorm flood disaster based on land use/land cover simulation, *Hydrological*
646 *Processes*, 36, e14771, <https://doi.org/10.1002/hyp.14771>, 2022.
- 647 [23] Irons, J. R., J. L. Dwyer, J. A. Barsi, 2012. The next Landsat satellite: the Landsat
648 data continuity mission. *Remote Sensing of Environment*, 122, 11-21.
649 <https://doi.org/10.1016/j.rse.2011.08.026>
- 650 [24] Jensen, S. K. and J. O. Domingue, 1998. Extracting Topographic Structure from
651 Digital Elevation Data for Geographic Information System Analysis.
652 *Photogrammetric Engineering and Remote Sensing*, 54(11), 1593-1600.
653 <https://doi.org/10.1109/36.7721>
- 654 [25] Jia, Y., G. Ni, and Y. Kawahara, 2001. Development of WEP model and its
655 application to an urban watershed. *Hydrol. Process.* 15: 2175–2194.
656 <https://doi.org/10.1002/hyp.275>
- 657 [26] Leopold, L. B., 1968. Hydrology for urban land planning--A guidebook on the
658 hydrologic effects of urban land use. *U.S. Geol. Surv. Circ.*, 554, 18 pp.
- 659 [27] Li, W., S. Chen, G. Chen, 2011. Urbanization signatures in strong versus weak
660 precipitation over the Pearl River Delta metropolitan regions of China.
661 *Environmental Research Letters* 6034020. [https://doi.org/10.1088/1748-](https://doi.org/10.1088/1748-9326/6/3/034020)
662 [9326/6/3/034020](https://doi.org/10.1088/1748-9326/6/3/034020).
- 663 [28] Li, Y., J. Zhang, R. Hao, et al., 2013. Effect of Different Land Use Types on Soil
664 Anti-scourability and Roughness in Loess Area of Western Shanxi Province.
665 *Journal of Soil and Water Conservation*, 27(4), 1-6.
666 <https://doi.org/10.13870/j.cnki.stbcxb.2013.04.016>
- 667 [29] Liang, X., D. P. Lettenmaier, E. F. Wood, and S. J. Burges, 1994. A simple
668 hydrologically based model of land surface water and energy fluxes for general
669 circulation models. *J. Geophys. Res.*, 99(D7), 14415-14428.
670 <https://doi.org/10.1029/94JD00483>
- 671 [30] Madsen, H., 2003. Parameter estimation in distributed hydrological catchment
672 modelling using automatic calibration with multiple objectives. *Advances in*
673 *Water Resources*, 26, 205-216. [https://doi.org/10.1016/S0309-1708\(02\)00092-1](https://doi.org/10.1016/S0309-1708(02)00092-1)
- 674 [31] O'Callaghan, J., and D. M. Mark, 1984. The extraction of drainage networks
675 from digital elevation data, *Comput. Vis. Graph. Image Process*, 28(3), 323-344.



- 676 [https://doi.org/10.1016/s0734-189x\(84\)80011-0](https://doi.org/10.1016/s0734-189x(84)80011-0)
- 677 [32] Pokhrel, P., K. K. Yilmaz, H. V. Gupta, 2012. Multiple-criteria calibration of a
678 distributed watershed model using spatial regularization and response signatures.
679 *J. Hydrol.*, 418-419, 49-602. <https://doi.org/10.1016/j.jhydrol.2008.12.004>
- 680 [33] Refsgaard, J.C., B. Storm, 1996. Construction, calibration and validation of
681 hydrological models. In: Abbott, M.B., Refsgaard, J.C. (Eds.), *Distributed*
682 *Hydrological Modelling*. Kluwer Academic, pp. 41-54.
683 https://doi.org/10.1007/978-94-009-0257-2_3
- 684 [34] Rose, S., N. E. Peters, 2001. Effects of urbanization on streamflow in the Atlanta
685 area (Georgia, USA): a comparative hydrological Approach. *Hydrological*
686 *Processes* 15(8), 1141-1157.
- 687 [35] Shafii, M. and F. D. Smedt, 2009. Multi-objective calibration of a distributed
688 hydrological model (WetSpa) using a genetic algorithm. *Hydrol. Earth Syst. Sci.*,
689 13, 2137-2149. <https://doi.org/10.5194/hessd-6-243-2009>
- 690 [36] Shen, S., S. Guze, 2007. Conversion Coefficient between Small Evaporation Pan
691 and Theoretically Calculated Water Surface Evaporation in China. *Journal of*
692 *Nanjing Institute of Meteorology*, 30(4), 561-565.
693 <https://doi.org/10.3354/ame01297>
- 694 [37] Smith, M. B., D.-J. Seo, V. I. Koren, S. Reed, Z. Zhang, Q.-Y. Duan, S. Cong, F.
695 Moreda, R. Anderson, 2004. The distributed model intercomparison project
696 (DMIP): motivation and experiment design. *J. Hydrol.*, 298 (1-4), 4-26.
697 <https://doi.org/10.1016/j.jhydrol.2004.05.001>
- 698 [38] Strahler, A. N., 1957. Quantitative Analysis of watershed Geomorphology.
699 *Transactions of the American Geophysical Union*, 35(6), 913-920.
700 <https://doi.org/10.1029/TR038i006p00913>
- 701 [39] Tang, H. Q., F. Xu, 2013. Analysis of new characteristics of the first Landsat 8
702 image and their Ecoenvironmental significance. *Acta Ecol. Sinica*, 33 (11), 3249-
703 3257. <https://doi.org/10.5846/stxb201305030912>
- 704 [40] Todini, E., 1996. The ARNO rainfall-runoff model. *J. Hydrol.* 175:339–382.
705 [https://doi.org/10.1016/S0022-1694\(96\)80016-3](https://doi.org/10.1016/S0022-1694(96)80016-3)
- 706 [41] Thiessen, A. H., 1911. Climatological data for July, 1911[J]. *Monthly Weather*
707 *Review*, 39:1082-1084.
- 708 [42] United Nations, 2014. World urbanization prospects: the 2014 revision :
709 highlights, 2014, New York, USA.
- 710 [43] Vapnik, V., 1995. *The Nature of Statistical Learning Theory*. Springer-Verlag,
711 New York. <https://doi.org/10.1007/978-1-4757-2440-0>
- 712 [44] Vieux, B. E., F. G. Moreda, 2003. Ordered physics-based parameter adjustment
713 of a distributed model. In: Duan, Q., Sorooshian, S., Gupta, H.V., Rousseau,
714 A.N., Turcotte, R. (Eds.), *Advances in Calibration of Watershed Models*. *Water*
715 *Science and Application Series*, vol. 6. American Geophysical Union, pp. 267-
716 281. <https://doi.org/10.1029/WS006p0267>
- 717 [45] Vieux, B. E., Z. Cui, and A. Gaur, 2004. Evaluation of a physics-based distributed
718 hydrologic model for flood forecasting. *Journal of Hydrology* 298:155-177, 2004.
719 <https://doi.org/10.1016/j.jhydrol.2004.03.035>

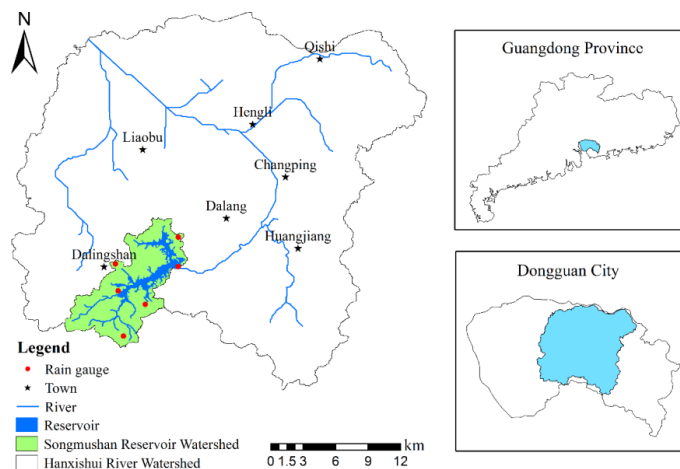


- 720 [46] Xu, H., Y. Chen, B. Zeng, J. He, Z. Liao, 2012. Application of SCE-UA
721 Algorithm to Parameter Optimization of Liuxihe Model. *Tropical Geography*,
722 32(1), 32-37. <https://doi.org/10.13284/j.cnki.rddl.001586>
- 723 [47] Xue, J., Wang, Q., and Zhang, M.: A review of non-point source water pollution
724 modeling for the urban–rural transitional areas of China: Research status and
725 prospect, *Science of The Total Environment*, 826, 154146,
726 <https://doi.org/10.1016/j.scitotenv.2022.154146>, 2022.
- 727 [48] Yang, L., Smith, J.A., Baeck, M.L., Zhang, Y., 2016: Flash flooding in small
728 urban watersheds: Storm event hydrologic response. *Water Resources Research*,
729 52 (6), pp. 4571-4589. <https://doi.org/10.1002/2015WR018326>
- 730 [49] Yu, B.: Ecological effects of new-type urbanization in China, *Renewable and*
731 *Sustainable Energy Reviews*, 135, 110239,
732 <https://doi.org/10.1016/j.rser.2020.110239>, 2021.
- 733 [50] Wang, H. and Chen, Y.: Identifying Key Hydrological Processes in Highly
734 Urbanized Watersheds for Flood Forecasting with a Distributed Hydrological
735 Model, 10.3390/w11081641, 2019.
- 736 [51] Wang, Y. H., Li, C. L., Liu, M., Cui, Q., Wang, H., Lv, J. S., Li, B. L., Xiong, Z.
737 P., and Hu, Y. M.: Spatial characteristics and driving factors of urban flooding in
738 Chinese megacities, *Journal of Hydrology*, 613, 10.1016/j.jhydrol.2022.128464,
739 2022.
- 740 [52] Zaradny, H., 1993. *Groundwater Flow in Saturated and Unsaturated Soil*. Now
741 York: A A Balkema.
- 742 [53] Zhang, S., D. Xu, Y. Li, 2006. An optimized inverse model used to estimate
743 Kostiakov infiltration parameters and Manning's roughness coefficient based on
744 SGA and SRFR model: I Establishment. *Shuili Xuebao* 37(11):1297-1302.
745 <https://doi.org/10.3321/j.issn:0559-9350.2006.11.003>
- 746 [54] Zhang, S., D. Xu, Y. Li, 2007. Optimized inverse model used to estimate Kostiakov
747 infiltration parameters and Manning's roughness coefficient based on SGA and
748 SRFR model: II Application. *Shuili Xuebao* 38(4):402-408.
749 <https://doi.org/10.13243/j.cnki.slx.2007.04.004>
- 750 [55] Zhang, H., Y. Chen, J. Zhou, 2015. Assessing the long-term impact of
751 urbanization on run-off using a remote-sensing-supported hydrological model.
752 *International Journal of Remote Sensing* 36(21): 5336-5352.
753 <https://doi.org/10.1080/01431161.2015.1094834>
- 754 [56] Zhang, M., Y. Liu, L. Wang, 2015. Inversion on Channel Roughness for
755 Hydrodynamic Model by Using Quantum-Behaved Particle Swarm
756 Optimization. *Yellow River* 37(2):26-29.
757 <https://doi.org/10.3969 /j.issn.1000-1379.2015.02.008>
- 758 [57] Zhao, R. J., 1977. *Flood Forecasting Method for Humid Regions of China*. East
759 China College of Hydraulic Engineering, Nanjing, China.
- 760 [58] Zhao, Y., Xia, J., Xu, Z., Qiao, Y., Shen, J., and Ye, C.: Impact of Urbanization
761 on Regional Rainfall-Runoff Processes: Case Study in Jinan City, China,
762 10.3390/rs15092383, 2023.

763
764



765 **Figures**

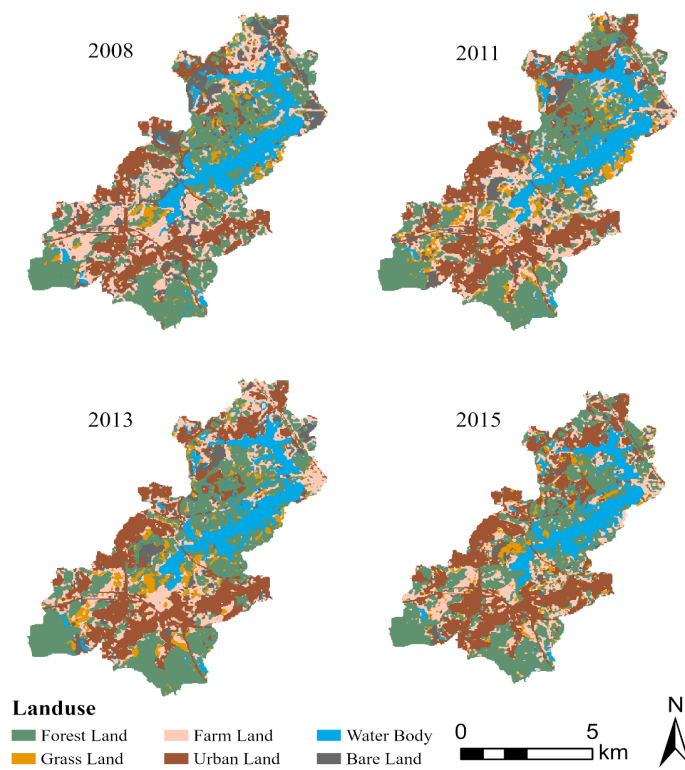


766

767

Fig. 1 Location of Songmushan Reservoir Watershed(SRW)

768



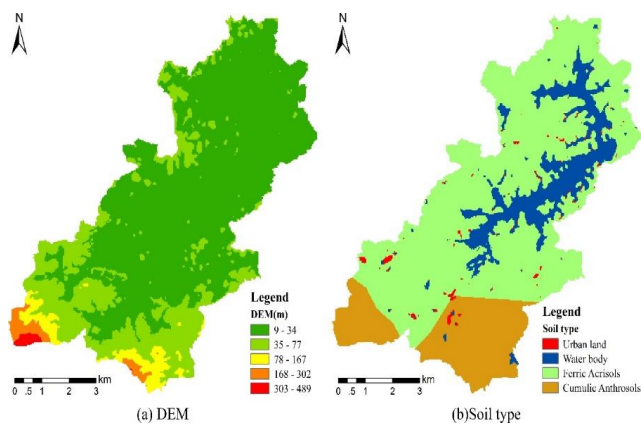
769

770

Fig. 2 LUCs of SRW



771

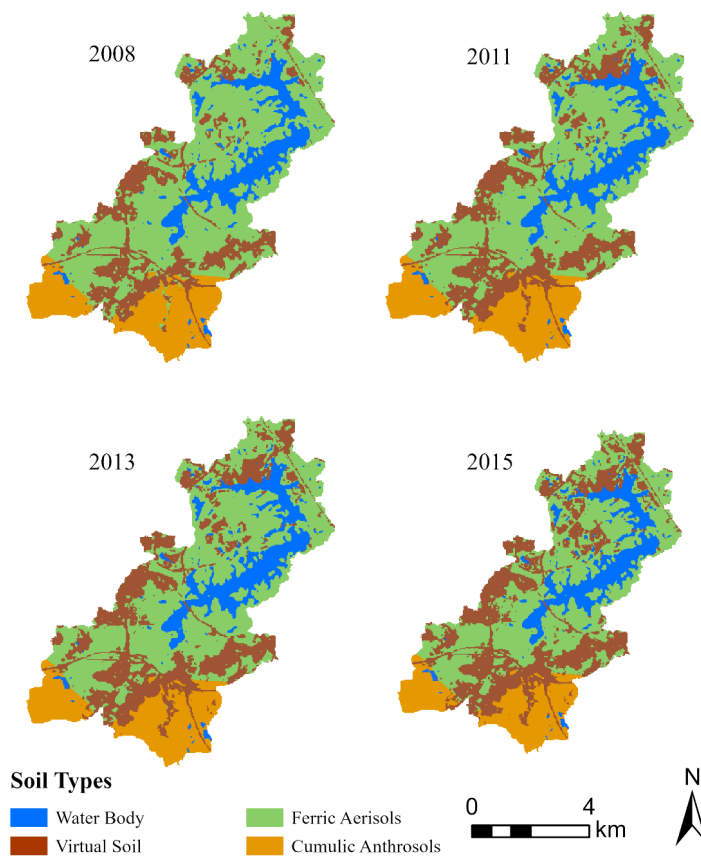


772

773

Fig. 3 Terrain property of SRW

774



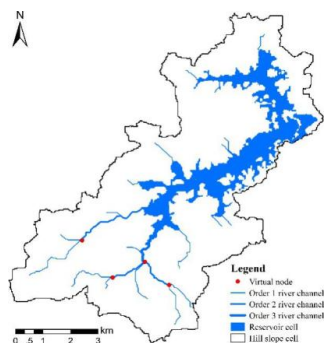
775

776

Fig. 4 Soil types of SRW adding urban land soil



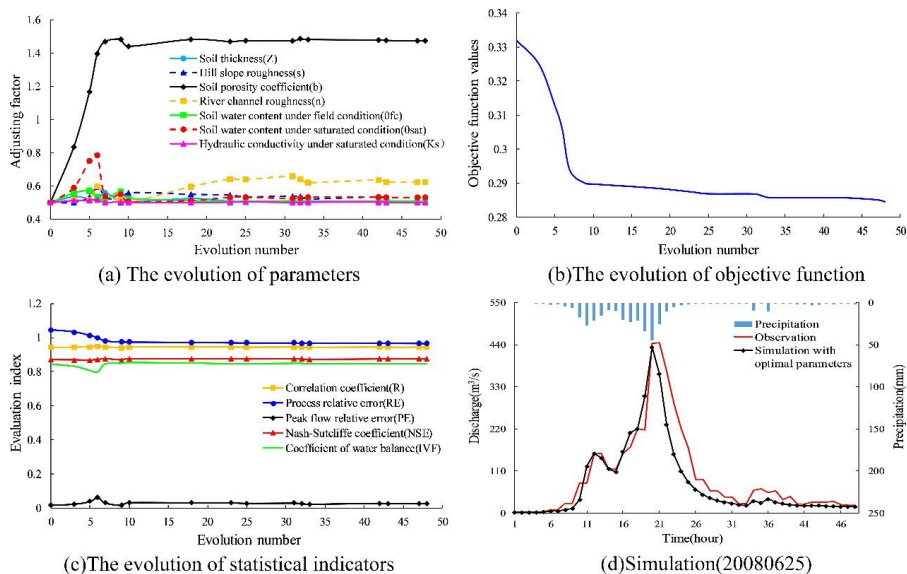
777



778
 779

Fig. 5 Structure of the Liuxihe model of SRW

780
 781

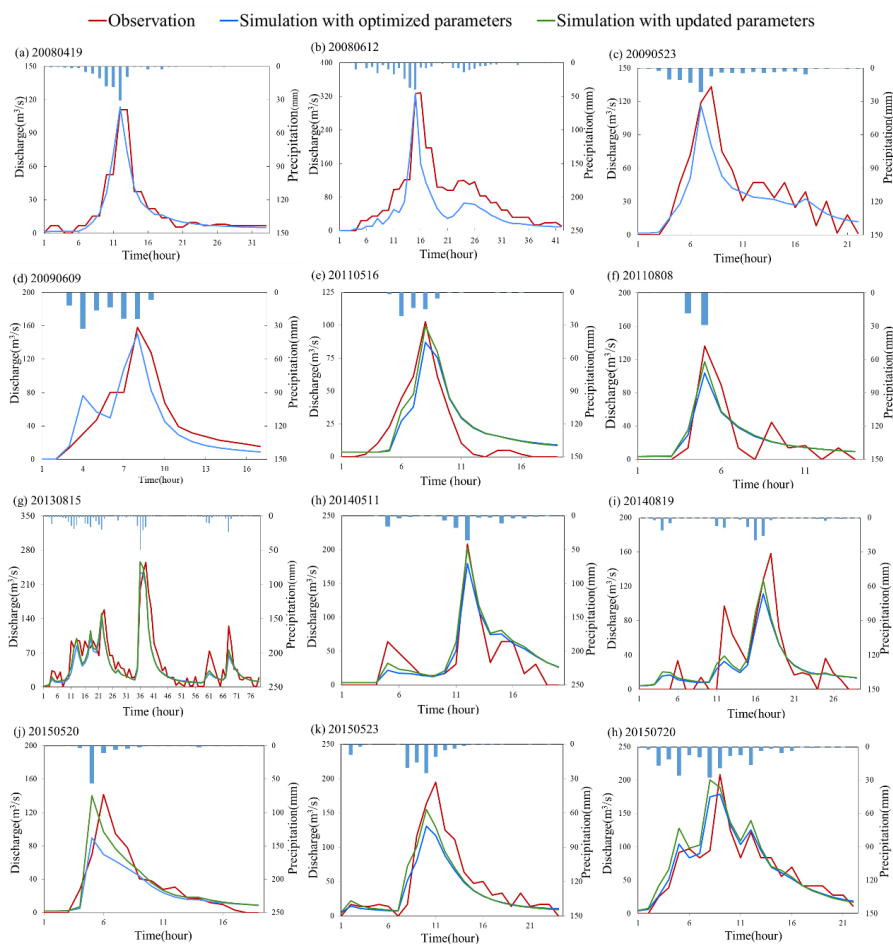


782

783

784

Fig. 6 results of parameter optimization



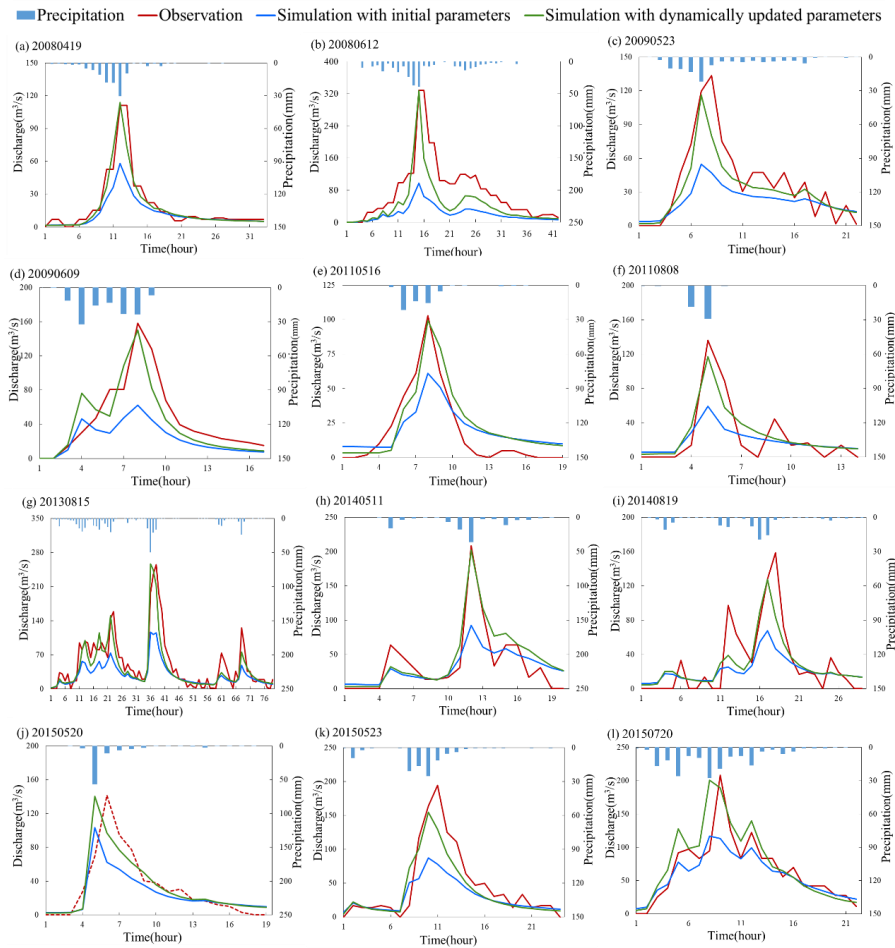
785

786 Fig. 7 Simulated flood hydrographs with Parameter-20080625-2008 and Parameter-

787

20080625-2008-updated

788



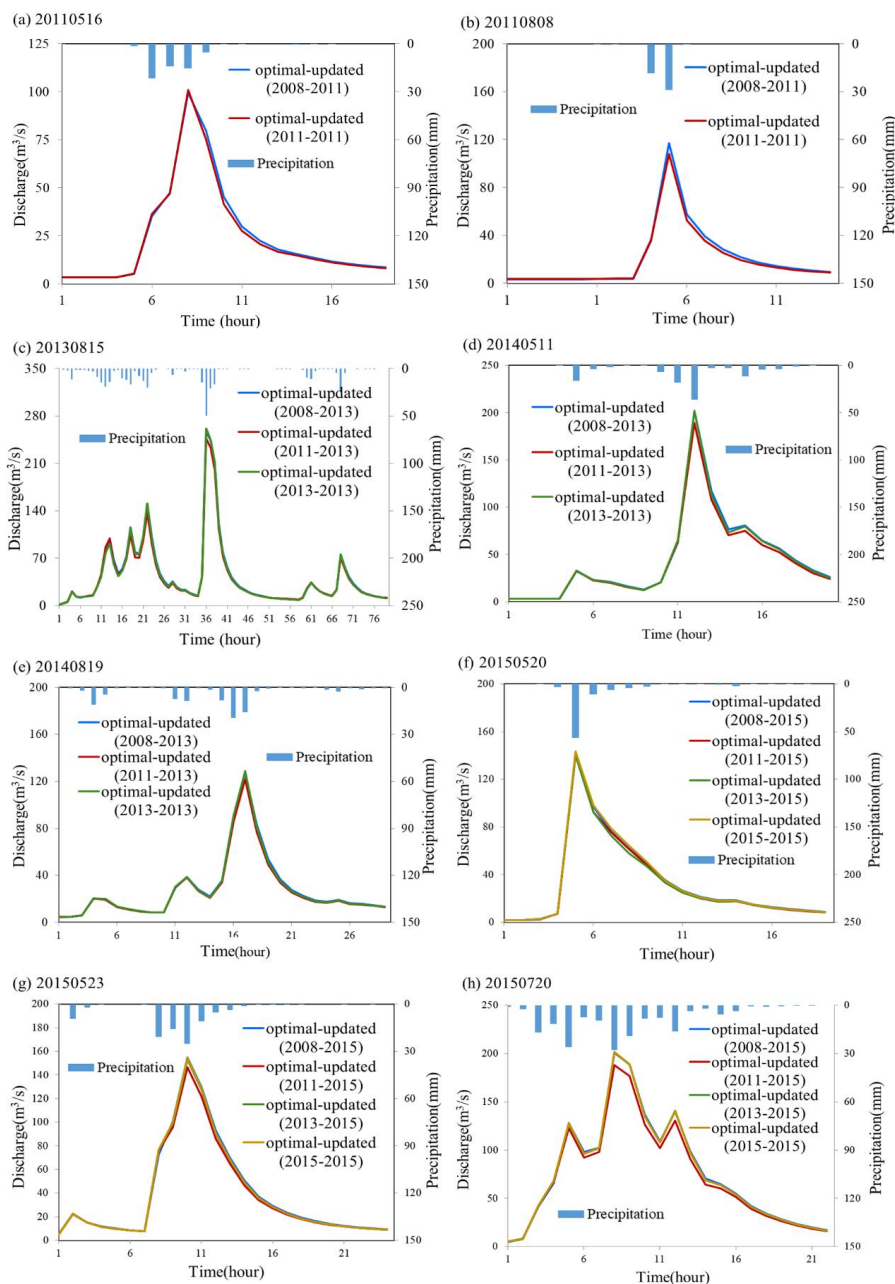
789

790 Fig. 8 Simulated flood hydrographs with initial parameter and dynamically updated

791

parameters

792



793

794 Fig. 9 Simulated flood hydrographs with dynamic parameter optimizing and updating.

795 * optimal-update (2008-2011) represents simulation results based on the 2008 LUC

796 optimization parameters and the 2011 LUC updated parameters.



797 **Tables**

798
 799

Table 1 Brief information of flood events

Flood event no.	Start time (yyyymmddhh)	End time (yyyymmddhh)	Total rainfall (mm)	Peak flow (m ³ /s)	Flood magnitude*
20080419	2008041910	2008042018	110.6	111.1	light
20080612	2008061219	2008061412	271.0	328.6	heavy
20080625	2008062500	2008062623	360.3	445.8	heavy
20090523	2009052304	2009052401	104.4	133.3	light
20090609	2009060900	2009060916	127.7	158.3	medium
20110516	2011051608	2011051702	60.1	102.8	light
20110808	2011080811	2011080900	48.6	136.1	light
20130815	2013081517	2013081823	351.3	254.7	heavy
20140511	2014051103	2014051122	110.7	208.3	medium
20140819	2014081914	2014082018	98.0	158.3	medium
20150520	2015052009	2015052103	90.1	141.7	light
20150523	2015052305	2015052404	100.9	194.4	medium
20150720	2015072022	2015072119	171.8	208.3	medium

800 * Flood magnitude is a qualitative measurement to the flood based on the peak flow of
 801 a flood event. I.e., for a flood event, if its peak flow is below 150 m³/s, then it's flood
 802 magnitude is light. On the other hand, if its peak flow is over 250 m³/s, it's flood
 803 magnitude is heavy. For other flood events, it's medium.

804
 805
 806

Table 2 Initial look-up table for vegetation-based parameters

Vegetation	Evaporation coefficient	Roughness
Forestry land	0.7	0.55
Grassland	0.6	0.18
Urban land	1.0	0.01
Bare land	0.4	0.12
Farmland	0.55	0.36

807
 808
 809



810

Table 3 Initial look-up table for soil-based parameters

Soil type	Soil water content under saturated conditions (%)	Soil water content under field capacity conditions (%)	Soil hydraulic conductivity under saturated conditions ($\text{mm}\cdot\text{h}^{-1}$)	Soil layer thickness (mm)
Urban land	0	0	0	0
Ferric Acrisols	46.1	26.5	20.78	1500
Cumulic Anthrosols	45.8	35.3	2.81	850

811

812 Table 4 Evaluation indices of simulated flood events with Parameter-20080625-2008

Flood event no.	Nash-Sutcliffe coefficient	Mean relative error (%)	Peak flow error (%)	Peak flow timing error/hour
20080419	0.93	31.29	0.49	0
20080612	0.70	38.83	0.94	-1
20090523	0.81	144.10	23.96	-1
20090609	0.90	24.60	1.41	0
20110516	0.77	189.10	15.27	0
20110808	0.78	52.65	56.48	0
20130815	0.80	97.98	7.71	-2
20140511	0.80	48.54	13.99	0
20140819	0.66	36.06	29.75	-1
20150520	0.69	43.34	36.58	-1
20150523	0.78	39.52	32.85	-1
20150720	0.81	20.87	14.19	0
average	0.79	63.91	19.47	-0.58

813

814

815

816

817

818

819

820

821

822

823

824

825

826

827

828

829

830



831 Table 5 Evaluation indices of simulated flood events with parameter-20080625-2008-
 832 updated

Flood event no.	Parameter	Nash-Sutcliffe coefficient	Correlation coefficient	Relative error (%)	Peak flow error (%)	Water balance coefficient	Peak flow timing error/hour
20110516	No-updated	0.769	0.889	189.10	15.30	1.17	0
	Updated	0.812	0.922	186.70	3.30	1.27	0
	Difference	0.043	0.033	-2.40	-12.00	0.10	0
	Increase(%)	5.600	3.700	1.27	-78.43	8.40	0
20110808	No-updated	0.784	0.919	57.30	23.80	1.01	0
	Updated	0.806	0.914	62.70	13.90	1.08	0
	Difference	0.022	-0.005	5.40	-9.90	0.07	0
	Increase(%)	2.800	-0.500	9.42	-41.60	7.10	0
20130815	No-updated	0.802	0.921	97.90	7.70	0.78	-2
	Updated	0.813	0.915	93.40	0.60	0.84	-2
	Difference	0.011	-0.006	-4.50	-7.10	0.05	0
	Increase(%)	1.400	-0.700	4.60	-92.21	6.90	0
20140511	No-updated	0.804	0.900	48.50	13.90	1.08	0
	Updated	0.819	0.921	52.40	3.00	1.20	0
	Difference	0.015	0.021	3.90	-10.90	0.11	0
	Increase(%)	1.900	2.300	8.04	-78.42	10.40	0
20140819	No-updated	0.659	0.865	36.10	29.80	0.83	-1
	Updated	0.689	0.849	33.60	19.50	0.92	-1
	Difference	0.030	-0.016	-2.50	-10.30	0.09	0
	Increase(%)	4.600	-1.800	6.93	-34.56	10.50	0
20150520	No-updated	0.691	0.873	43.30	36.60	0.80	-1
	Updated	0.683	0.837	46.20	0.90	1.01	-1
	Difference	-0.008	-0.036	2.90	-35.70	0.21	0
	Increase(%)	-1.200	-4.100	6.70	-97.54	26.40	0
20150523	No-updated	0.782	0.959	39.50	32.80	0.73	-1
	Updated	0.823	0.932	42.60	20.40	0.83	-1
	Difference	0.041	-0.027	3.10	-12.40	0.09	0
	Increase(%)	5.200	-2.800	7.85	-37.80	12.70	0
20150720	No-updated	0.810	0.914	20.90	14.20	1.05	0
	Updated	0.666	0.889	29.70	3.70	1.15	-1
	Difference	-0.144	-0.025	8.80	-10.50	0.10	-1
	Increase(%)	-17.800	-2.700	42.11	-73.94	9.70	0
average	No-updated	0.763	0.905	66.58	21.76	0.93	-0.63
	Updated	0.764	0.897	68.41	8.16	1.03	-0.75
	Difference	0.001	-0.008	1.84	-13.60	0.10	-0.13
	Increase(%)	0.313	-0.825	10.86	-66.81	11.51	20.00

833

834

835

836

837

838

839



840 Table 6 The evaluation indices of simulated flood events with initial and dynamically
 841 updated parameters

Flood event no.	Parameter	Nash-Sutcliffe coefficient	Mean relative error (%)	Peak flow error (%)	Peak flow timing error/hour
20080419	initial	0.604	0.310	0.507	0
	updated	0.928	0.313	0.005	0
	difference(%)	53.6	1.0	-99.0	0.0
20080612	initial	0.010	0.559	0.708	-1
	updated	0.701	0.388	0.009	-1
	difference(%)	6910.0	-30.6	-98.7	0.0
20090523	initial	0.304	1.489	0.628	-1
	updated	0.809	1.441	0.239	-1
	difference(%)	166.1	-3.2	-61.9	0.0
20090609	initial	0.335	0.385	0.611	0
	updated	0.897	0.246	0.014	0
	difference(%)	167.8	-36.1	-97.7	0.0
20110516	initial	0.636	1.831	0.481	0
	updated	0.812	1.867	0.033	0
	difference(%)	27.7	2.0	-93.1	0.0
20110808	initial	0.482	0.526	0.568	0
	updated	0.806	0.627	0.139	0
	difference(%)	67.2	19.2	-75.5	0.0
20130815	initial	0.476	1.038	0.543	-2
	updated	0.813	0.934	0.006	-2
	difference(%)	70.8	-10.0	-98.9	0.0
20140511	initial	0.548	0.432	0.556	0
	updated	0.819	0.524	0.030	0
	difference(%)	49.5	21.3	-94.6	0.0
20140819	initial	0.398	0.412	0.573	-1
	updated	0.689	0.336	0.195	-1
	difference(%)	73.1	-18.4	-66.0	0.0
20150520	initial	0.576	0.513	0.269	-1
	updated	0.683	0.462	0.009	-1
	difference(%)	18.6	-9.9	-96.7	0.0
20150523	initial	0.518	0.413	0.550	-1
	updated	0.823	0.426	0.204	-1
	difference(%)	58.9	3.1	-62.9	0.0
20150720	initial	0.724	0.222	0.439	-1
	updated	0.666	0.297	0.037	-1
	difference(%)	-8.0	33.8	-91.6	0.0
average	initial	0.468	0.678	0.536	-0.667
	updated	0.787	0.655	0.077	-0.667
	difference(%)	68.2	-2.3	-86.4	0.0

842

843

844



845 Table 7 Evaluation indices of simulated flood events with dynamic parameter
 846 optimizing and updating

Flood event no.	Optimizing year	Nash-Sutcliffe coefficient	Correlation coefficient	Relative error (%)	Peak flow error (%)	Water balance coefficient	Peak flow timing error/hour
20110516	2008	0.812	0.922	1.867	0.033	1.269	0
	2011	0.845	0.934	1.724	0.019	1.231	0
20110808	2008	0.806	0.914	0.627	0.139	1.076	0
	2011	0.780	0.909	0.621	0.206	0.997	0
20130815	2008	0.813	0.915	0.934	0.006	0.838	-2
	2011	0.789	0.909	0.962	0.032	0.799	-2
	2013	0.797	0.908	0.922	0.028	0.822	-2
20140511	2008	0.819	0.921	0.524	0.030	1.195	0
	2011	0.839	0.923	0.487	0.091	1.127	0
	2013	0.828	0.923	0.512	0.031	1.181	0
20140819	2008	0.689	0.849	0.336	0.195	0.918	-1
	2011	0.662	0.844	0.329	0.231	0.871	-1
	2013	0.675	0.841	0.332	0.186	0.904	-1
20150520	2008	0.683	0.837	0.462	0.009	1.006	-1
	2011	0.663	0.825	0.451	0.006	0.979	-1
	2013	0.658	0.821	0.455	0.009	0.966	-1
	2015	0.677	0.837	0.455	0.011	1.018	-1
20150523	2008	0.823	0.932	0.426	0.204	0.826	-1
	2011	0.776	0.918	0.465	0.246	0.784	-1
	2013	0.803	0.923	0.452	0.211	0.814	-1
	2015	0.806	0.923	0.449	0.207	0.816	-1
20150720	2008	0.666	0.889	0.297	0.037	1.151	-1
	2011	0.721	0.883	0.288	0.097	1.084	-1
	2013	0.659	0.885	0.304	0.033	1.144	-1
	2015	0.657	0.885	0.304	0.032	1.145	-1

847
 848
 849

Table 8 impact of urbanization on peak flow

Flood event no.	Peak flow (m ³ /s)			Urbanization rate (%)*		
	no-update	update	increase(%)	no-update	update	increase(%)
20110516	87.08	99.42	14.2	18.62	23.4	25.67
20110808	103.68	117.21	13.1	18.62	23.4	25.67
20130815	235.08	256.19	9.0	18.62	26.24	40.92
20140511	179.18	202.07	12.8	18.62	26.24	40.92
20140819	111.23	127.43	14.6	18.62	26.24	40.92
20150520	89.85	140.44	56.3	18.62	30.37	63.10
20150523	130.58	154.72	18.5	18.62	30.37	63.10
20150720	178.78	200.59	12.2	18.62	30.37	63.10

850 *Urbanization rate is the rate of urban land area to the whole watershed area.
 851
 852
 853